Int. J. Heat Mass Transfer. Vol. 25, No. 12, pp. 1885-1894, 1982
Printed in Great Britain

0017-9310/82/121885-10 $03.00/0
Pergamon Press Ltd.

ON THE DEFORMATION OF THE RECTANGULAR TURBULENT JET CROSS-SECTION

G. N. ABRAMOVICH
Moscow Aviation Institute, Moscow, U.S.S.R.

(*Received* 22 *September* 1981)

Abstract—The paper explains the reason for the experimentally observable deformation of a rectangular turbulent jet manifesting itself in a rapid growth (along the jet length) of the jet cross-section short side and a reduction of its long side. As a result, these sides change places some distance downstream of the jet origin. The jet deformation is shown to be due to a specific pressure field induced by large vortices that originate in the jet mixing zone.

A method of calculating the jet deformation is developed which makes use of the author's information on the pressure field produced by large vortices. The predicted results are compared with the experimental data available from other sources. The theory suggested applies to jet flows in boiler furnaces, dryers, combustion chambers of jet engines and stationary gas-turbine plants of electric power stations, chemical reactors, etc.

NOMENCLATURE

- a, b, cross-section sides (inside of vortex);
- A_0, dimensionless circulation of vortex;
- p, static pressure;
- r_0, vortex cross-section radius;
- t, time;
- u, averaged flow velocity;
- U, mean relative velocity of fluctuating flow past a vortex;
- V, deformation rate of jet cross-section;
- x, longitudinal coordinate;
- R, side of an equivalent square, $(ab)^{1/2}$;
- y, transverse coordinate;
- y_0, distance between axes of subtending segments of vortex.

Greek symbols

- δ, jet mixing layer thickness;
- Γ, vortex circulation;
- Δ, difference sign;
- ρ, density.

Subscripts

- 0, vortex axis;
- a, direction of long side of initial cross-section;
- b, direction of short side of initial cross-section;
- jb, free (vortex);
- i, induced (velocity); starting portion;
- ia, ib, end of jet starting portion;
- K, constricted jet cross-section;
- m, jet axis;
- tr, end of transitional portion of jet.

1. INTRODUCTION

THE STUDY of turbulent rectangular jets has been the concern of many Soviet and foreign investigations for almost 50 years. The first experimental work, in which the averaged velocity fields were studied in rectangular jets with initial cross-section side ratios of 1, 2, 5 and 10, was carried out in the U.S.S.R. in 1933 [1].

During the ensuing 30 years the interest both of Soviet and foreign scientists was centered around studying a plane-parallel turbulent jet. Different semi-empirical theories of a plane jet have been developed. They are summarized in ref. [2]. In experiments, particular attention has been paid to the provision of such experimental conditions which would preclude, wherever possible, the 'spatial effect' (e.g. by using special screens) [3, 4].

The mid-1960s again saw the advent of studies devoted to 3-dim. jets and wakes [5, 6]. A thorough experimental investigation of rectangular jets was carried out by Krashennikov and Rogalskaya [7] who noted a strong effect of initial efflux conditions on the intensity of subsequent jet deformation.

In recent years, attempts have been made to calculate the strained rectangular jet [8] based on the assumption of the existence of substantial transverse velocity components over the circumference of a rectangular jet. However, these studies lack a sufficient physical justification for the abnormal transverse velocities and, therefore, the approach applied is artificial in character.

In the present paper, a hypothesis is advanced that large vortices, which are formed in the turbulent mixing zone, are responsible for the occurrence of an oscillating pressure field. The time-average pressure depends on the relative distance between parallel segments of a closed large vortex located at the jet cross-section. The closer the segments are to the jet axis and the thicker these vortex segments are, the lower is the mean pressure at the given point of the inner vortex field. Therefore, the shorter and more widely spaced sides of the fluid contour, embraced by a closed rectangular vortex, experience a higher pressure than its longer sides. This induces an overflow of fluid in the jet cross-section plane, which results in a gradual deformation of the vortex, its internal field, and of the whole jet cross-section.

The approximate theory of the effect of large vortices on turbulent jet structure, developed earlier by the author [10, 13], allows the determination of the relative thickness of a vortex, relative distances between the opposite vortex segments, and, respectively, the time-average pressure field. Making use of this information and relating the pressure distribution to a straining transverse fluid motion, a physically sound technique is suggested for the approximate calculation of rectangular jet deformation, which shows a satisfactory agreement with the experimental data published between 1973 and 1979 [7, 9, 10, 11].

2. PRESSURE FORCES AT THE CROSS-SECTION

Let us consider the reasons for the deformation of a 3-dim. jet. Experiments [5–11] show that spreading of a turbulent rectangular submerged jet is accompanied by deformation of its cross-section, with the smaller side of the rectangle increasing in a streamwise direction and the larger side decreasing. At a certain distance from the jet origin, its cross-section acquires a square shape (with rounded corners), but this shape is only an intermediate one. Farther away from the jet origin, the directions of the short and long sides of the jet cross-section change places (Fig. 1). Presumably if this process had not been influenced by turbulent mixing, then at some distance from the origin the jet would have acquired the cross-section of the initial rectangular form, but located at 90° to the initial cross-section. After that the direction of deformation would have been reversed. However the turbulent mixing leads to the decay of variations of the rectangular jet cross-section shape.

It follows from refs. [10, 11] that large vortices originate in the mixing layers and are transported by an averaged flow at the velocity equal to the local averaged velocity u_0. The fluctuating portion of the flow moves past these vortices at the relative velocity, which is porportional to the maximum eddy velocity $U \sim \langle u'_0 \rangle$ (Fig. 2). The pressure field, resulting from the fluctuating flow past large vortices, moves with the same averaged velocity u_0 as the large vortices, i.e. constitutes a travelling pressure wave. It moves at the velocity $u_0 - u$ relative to any flow layer having the velocity u.

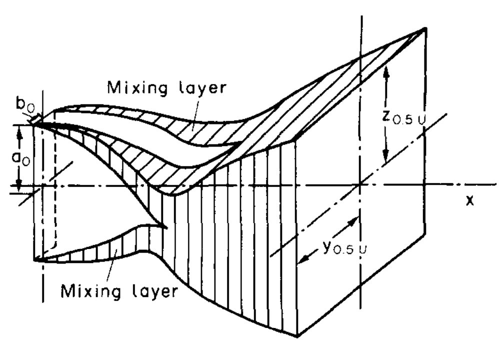

FIG. 1. Configuration of a rectangular jet.

The pressure fields produced by large vortices have been obtained [10, 11]. Thus, over the trajectory traversed by a large vortex in a plane jet the maximum instantaneous deviation of pressure from that observed in an undisturbed surrounding fluid is

$$\langle p'_0 \rangle_{\max} = 0.5\rho_0 U^2[1 - (1+q)^2] = -0.5\rho_0 U^2(2q + q^2) \quad (1)$$

where

$$q = \frac{1 + [r_0/(2y_0 + r_0)]^2 \pm [Ar_0/2\delta][\pm 1 - r_0/(2y_0 + r_0)]}{1 - 0.25[(r_0/y_0)^2 \pm A_0 r_0^2/\delta y_0]}. \quad (2)$$

The magnitude of the dimensionless parameter q depends on the vortex radius r_0, mixing layer thickness δ, spacing between the axes of a pair of opposite vortices located at a jet cross-section y_0 (Fig. 2), and the dimensionless vortex circulation A_0.

In ref. [10], the following quantities were used

$$r_0 = K_1\delta, \quad A_0 = \frac{\delta|\Gamma|}{\pi r_0^2 U}. \quad (3)$$

Here $K_1 = 0.22$ is the empirical constant, $A_0 = 2$ over the initial portion of the jet, $A_0 = 2.27$ over the transitional and main portions. According to ref. [10], the maximum relative velocity is equal to one quarter of the maximum averaged velocity at the jet cross-section: $U = 0.25\,u_m$. The average pressure fluctuation on the line of motion of large vortices is shown there to be about one fifth of its maximum value

$$\langle p'_0 \rangle = 0.22\langle p'_0 \rangle_{\max}.$$

Substitution of all of the above values into equation (1) yields the formula for the mean deviation from the non-perturbed gas pressure on the vortex line

$$\langle p'_0 \rangle = -0.008\,\rho_0 u_m^2(2q + q^2). \quad (4)$$

Let us assume that in a rectangular jet the ends of vortices, originating in mutually perpendicular mixing layers, converge and form a closed cylindrical vortex rolled up as a rectangle (Fig. 3). In this case, as follows from equation (4), the more closely spaced opposite segments of vortices ($y_{0b} = b$) induce a higher rarefaction. The difference of pressures on the sides of the rectangular inner field encompassed by the vortex induces a straining motion, the streamlines of which are shown in Fig. 4. This straining motion results in gradual shortening of the long side, and lengthening of the short side, of rectangular jet cross-section. At the location where the cross-section becomes square ($a = b$), the pressures at the sides a and b balance out, but the straining motion persists by inertia until the increasing pressure difference, which reverses its sign at $b > a$, completely decelerates the process of defor-

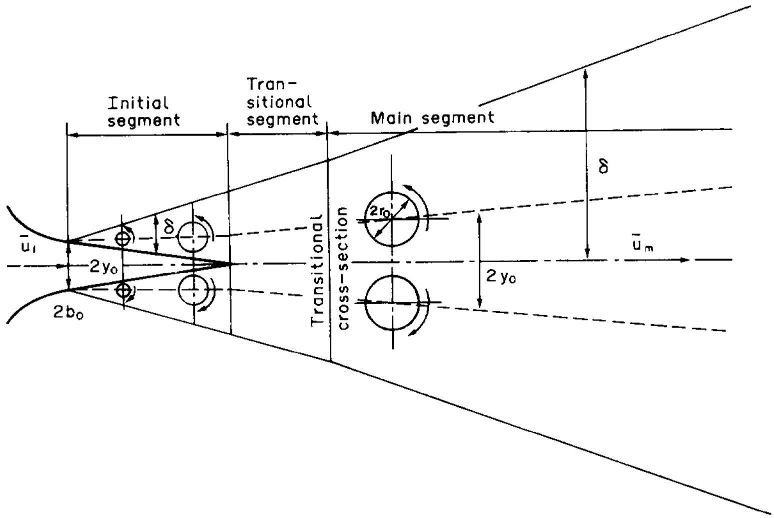

FIG. 2. Schematic of a jet.

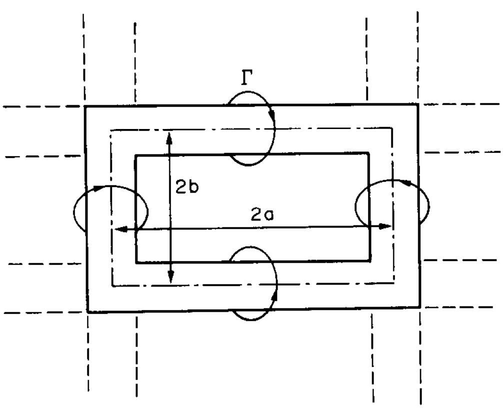

FIG. 3. A closed vortex at the rectangular jet cross-section.

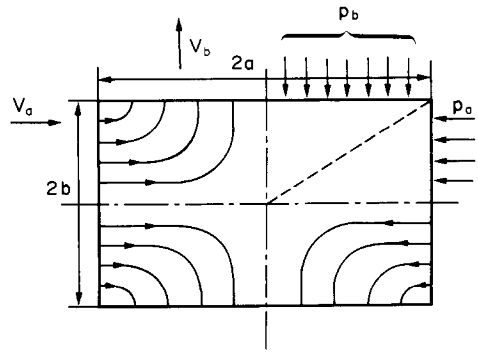

FIG. 4. Stream lines in straining motion.

mation, following which the next cycle of jet cross-section deformation starts and so on.

3. RATES OF CROSS-SECTION DEFORMATION

The following method of calculation of the 3-dim. jet deformation is suggested. We shall determine the difference of pressures applied to the sides $2a$ and $2b$ of a rectangular inner vortex field based on the assumption that the vortex segments located at these sides act as infinite vortices, i.e. we shall extend equation (4) to the segments of a rectangular vortex. Then the mean differences of pressures applied to short and long sides of a rectangular inner vortex field, respectively, is

$$\Delta p = \langle p'_{0b} \rangle - \langle p'_{0a} \rangle = 0.008\, \rho_0 u_m^2 (q_a - q_b)(2 + q_a + q_b). \quad (5)$$

We substitute $y_{0b} = b$ into equation (2) when determining q_b and $y_{0a} = a$ when determining q_a.

The straining motion of an incompressible fluid in the jet cross-section plane can be calculated based on the following considerations (Fig. 4). The area encompassed by a rectangular vortex does not change on deformation of the cross-section over a short segment of the jet equal to the calculation step Δx.

In the initial cross-section of the jet

$$R_0^2 = ab = a_0 b_0 = \text{const.} \quad (6)$$

According to the continuity condition, the instantaneous values of the deformation rate on the mutually perpendicular sides of rectangular cross-section are

$$V_a b = -V_b a \quad (7)$$

where

$$V_a = \mathrm{d}a/\mathrm{d}t, \quad V_b = \mathrm{d}b/\mathrm{d}t.$$

The total work of pressure forces (over an infinitely short interval of time $\mathrm{d}t$) applied to the mass of fluid filling the rectangular cross-section is equal to a change in the total kinetic energy of this mass

$$-\mathrm{d}L_p = \langle p'_{0b} \rangle a V_b \mathrm{d}t + \langle p'_{0a} \rangle b V \mathrm{d}t = 0.25\, ab\, \rho_0 \mathrm{d}(V_a^2 + V_b^2). \quad (8)$$

Here, an assumption has been used that one half of the considered mass, which lies above the diagonal of the rectangular cross-section quarter (Fig. 4), has the velocity V_b, while that lying below, the velocity V_a.

The quantities $\langle p'_{0b} \rangle$ and $\langle p'_{0a} \rangle$, obtained from equation (4), are mean pressures at the respective sides of the rectangular cross-section. The use of equations (5), (6) and (7) reduces equation (8) to the following form:

$$- \Delta p = \frac{1}{2} \rho_0 \left(b \frac{\mathrm{d}V_b}{\mathrm{d}t} - a \frac{\mathrm{d}V_a}{\mathrm{d}t} \right) \quad (9)$$

where, according to equations (6) and (7),

$$\frac{\mathrm{d}V_b}{\mathrm{d}t} = \frac{\mathrm{d}^2 b}{\mathrm{d}t^2}, \quad \frac{\mathrm{d}V_a}{\mathrm{d}t} = \frac{\mathrm{d}^2 a}{\mathrm{d}t^2} = a \left[\frac{2}{b^2} \left(\frac{\mathrm{d}b}{\mathrm{d}t} \right)^2 - \frac{1}{b} \frac{\mathrm{d}^2 b}{\mathrm{d}t^2} \right]. \quad (10)$$

Substituting equation (10) into equation (9) and accounting for equations (6) and (7), we have

$$-\Delta p = 0.5 \rho_0 \left[\left(b + \frac{a^2}{b} \right) \frac{\mathrm{d}^2 b}{\mathrm{d}t^2} - \frac{2a^2}{b^2} \left(\frac{\mathrm{d}b}{\mathrm{d}t} \right)^2 \right]. \quad (11)$$

It follows from equation (11) that in the initial cross-section of the jet, when $V_b = \mathrm{d}b/\mathrm{d}t = 0$, the acceleration of straining motion is

$$\left(\frac{\mathrm{d}^2 b}{\mathrm{d}t^2} \right)_0 = \frac{2 \Delta p}{\rho_0 \left[b_0 + (a_0^2 / b_0) \right]}.$$

At the distance x_q from the jet origin, where the field encompassed by the vortex becomes square ($a = b$, $V_{bq} = V_{aq}$, $\Delta p_q = 0$)

$$\left(\frac{\mathrm{d}^2 b}{\mathrm{d}t^2} \right)_q = - \frac{V_{bq}^2}{b_q}.$$

At the end of the first 'half-wave' of deformation ($x = x_K$), when again $V_{bK} = 0$

$$\left(\frac{\mathrm{d}^2 b}{\mathrm{d}t^2} \right)_K = \frac{2 \Delta p_K}{\rho_0 [b_K + a_K^2 / b_K)]}.$$

Over the length where $x < x_q$, $\Delta p < 0$, and over the length with $x_q < x < x_K$, $\Delta p > 0$. In the general form equation (11) yields

$$\left(\text{taking into account} \frac{\mathrm{d}b}{\mathrm{d}t} = V_b = - V_a \frac{b}{a} \right)$$

$$\frac{\mathrm{d}^2 b}{\mathrm{d}t^2} = \frac{2(\Delta p / \rho_0 - V_a^2)}{b + a^2 / b} = \frac{2(\Delta p / \rho_0 - V_a^2)}{b + R^4 / b^3}. \quad (12)$$

Owing to the fact that calculation of different portions of a deforming jet (initial, transitional and main) is characterized by specific features, we shall consider each portion in detail.

4. CALCULATION METHOD

It is known from the theory of turbulent jets [2], that the starting portion of the jet is equal to about 9 initial half-widths for a plane-parallel jet (at $a_0 \to \infty$) or to 9 initial radii for a round jet. A specific feature of the rectangular jet is the non-simultaneous penetration of the mixing layers, formed at its side surfaces, to the jet axis.

We shall assume that the mixing layer thickness over the starting portion of a rectangular jet is uniform over the whole perimeter of any cross-section and increases along the jet [2] by the law

$$\delta = 0.27\, x. \quad (13)$$

The abscissa x_{ib} (at $b < a$) of the point, where the boundary of the mixing layer maximum velocity first intersects the rectangular jet axis, is determined from

$$y_{ib} = b_i, \quad (14)$$

where b_i is found by successive calculation of the jet divided into steps of equal length Δx.

It is shown in refs. [10, 11] that over the starting portion of an ordinary jet, large vortices move along the line which continues the edge of the nozzle, in view of which the transverse distance between the opposite vortices remains the same and equal to the nozzle width. In the case of a rectangular jet, it is logical to assume that over the jet starting portion at $x < x_{ib}$, a large vortex encompasses a rectangular field of constant area ($ab = a_0 b_0 = R_0^2$).

It is recommended that deformation of the starting portion of a rectangular jet be calculated in the following sequence. Having chosen the calculation step Δx, determine the time required for a vortex to traverse this step

$$\Delta t = \Delta x / u_0 \quad (15)$$

where $u_0 = 0.7\, u_1$ is the rate of vortex displacement, u_1 is the velocity in the jet core equal to the velocity of discharge. Hence,

$$\Delta t = 1.43\, \Delta x / u_1. \quad (16)$$

Then, equation (12) yields the rate of deformation

$$V_b = \frac{\mathrm{d}b}{\mathrm{d}t} = \left(\frac{\mathrm{d}^2 b}{\mathrm{d}t^2} \right) \Delta t. \quad (17)$$

The acceleration $\mathrm{d}^2 b / \mathrm{d}t^2$ is determined from equations (5) and (2) for the local values of pressure difference at the adjacent sides of the rectangular field of a vortex, with $y_{0a} = a$, $y_{0b} = b$, $r_0 = 0.22\,\delta$ and $V_a = V_b(a/b)$ for the nth step being taken from calculations of the previous $(n - 1)$th step. At the jet origin, i.e. for the first step, the deformation rates are equal to zero ($V_a = V_b = 0$). As noted, the area of the inner vortex field at $x < x_{ib}$ is taken to be constant ($R_0 = a_0 b_0$). The increment in the mixing layer thickness at the distance of one step, in accordance with equation (13), is

$$\Delta \delta = 0.27\, \Delta x. \quad (18)$$

According to equation (17), the increment in the small side of a rectangular vortex field is

$$\Delta b = V_b \mathrm{d}t = \left(\frac{\mathrm{d}b}{\mathrm{d}t} \right) \Delta t. \quad (19)$$

From this

$$b_n = b_{n-1} + \Delta b_n \tag{20}$$

and, after equation (6),

$$a_n = \frac{R_0^2}{b_n}. \tag{21}$$

It has been shown [10] that the vortex axis is located at the distance

$$y_n = 0.3\,\delta_n \tag{22}$$

from the boundary of the mixing layer maximum velocity. Therefore, the longitudinal coordinate x_{ib} of the cross-section, at which the mixing layer intersects the jet axis, is sought in the process of calculation from the condition

$$y_{ib} = b_{ib} = 0.3\,\delta_{ib}. \tag{23}$$

Calculation of the transitional portion of the jet requires additional explanations. In the mixing layers carrying long segments of the rectangular vortex, between the point $x = x_{ib}$ and the point, where the adjacent mixing zone intersects the jet axis ($x = x_{ia}$), the flow pattern sets in, which is representative of the transitional section, while in the remainder two layers (that have failed to reach the jet axis) the starting-portion mode of flow is maintained. In connection with this, in the zone $x > x_{ib}$ the equality of thicknesses of the adjacent mixing layers is violated ($\delta_a \neq \delta_b$). The increment in the layer thickness δ_a can, as before, be determined from equation (18)

$$\Delta\delta_a = 0.27\,\Delta x,$$

while the thickness of the adjacent layer δ_b should be sought in this zone following the laws of transitional portion of the jet, i.e. according to ref. [2], as

$$\Delta\delta_b = 0.18\Delta x. \tag{24}$$

The parameters q_a and q_b are calculated using different values of y_0 determined respectively for the mixing layer adjacent to the jet axis from condition (22)

$$y_{0b} = 0.3\,\delta_b, \tag{25}$$

and for the mixing layer bordering on the constant velocity zone from

$$y_{0a} = a. \tag{26}$$

Moreover, over the portion $x > x_{ib}$, according to equation (25), it is necessary to account for a one-sided increase in the vortex field, with an increment in R in equations (6) and (12) over the length Δx being determined according to equations (24)–(26) as

$$\Delta(R^2) = a_0\Delta b = 0.3\Delta\delta_b a_0 = 0.054 a_0 \Delta x. \tag{27}$$

The calculation is allowed to progress till the second mixing layer comes close to the jet axis ($x = x_{ia}$). If at $x_{trb} < x_{ia}$ the transitional portion terminates in the layer δ_b, then in the zone $x_{trb} < x < x_{ia}$ it will behave just as in the main portion of the jet; then equation (24) is to be replaced by [2]

$$\Delta\delta_b = 0.22\Delta x, \tag{28}$$

and then, in place of equation (27), we obtain

$$\Delta(R^2) = 0.066 a_0 \Delta x. \tag{29}$$

Corresponding to different thicknesses of mixing layers ($\delta_a \neq \delta_b$) there are different radii of large vortex segments ($r_{0a} \neq r_{0b}$) and, consequently, different values of circulation ($\Gamma_a \neq \Gamma_b$) that are determined by equation (3) as

$$\Gamma_a = \pi r_{0a}^2\, U A_0/\delta_a, \quad \Gamma_b = \pi r_{0b}^2 U A_0/\delta_b. \tag{30}$$

At the corners of the jet cross-section where the ends of adjacent segments of the vortex join together, a jump in circulation takes place

$$\Delta\Gamma_{jb} = \Gamma_a - \Gamma_b = \Gamma_b(\delta_a/\delta_b - 1). \tag{31}$$

It is evident that this results in the development of the following vortex system. A closed vortex of smaller circulation Γ_b is located in the cross-section, while the ends of the vortex of larger circulation Γ_a are split into two parts: one part enters the closed vortex, while the other, corresponding to the excess of circulation $\Delta\Gamma_{jb}$, forms a free end of the vortex entering the zone of reduced velocity where the relative motion of fluid carries it away along the path of the jet. The end of the free vortex should rest in this case on the exit edge of the jet nozzle, which provides the fulfillment of the condition of vortex conservation. The vortex system described, which is shown in Fig. 5, is similar to that formed on the finite span wing.

Free vortices induce additional velocities V_{ai} and V_{bi} that influence the process of jet deformation.

Thus, besides the velocities V_a and V_b determined on the basis of pressure differences, calculation of jet deformation over the transitional portion should include the induced velocities, i.e. it should be assumed that

$$V_{a\Sigma} = V_a \pm V_{ai}, \quad V_{b\Sigma} = V_b \pm V_{bi}. \tag{32}$$

The sign depends on the direction of induced velocity. In order to determine the mean value of the induced velocity (on the given side of the cross-section), formulae from the finite-span wing theory can be used

$$V_{ai} = \Delta\Gamma_{jb}/(\pi a) \tag{33}$$

and similarly

$$V_{bi} = \Delta\Gamma_{jb}/(\pi b). \tag{34}$$

Here, the circulation of a free vortex is determined from equations (30) and (31) as

$$\Delta\Gamma_{jb} = (\pi r_{0b}^2\, U A_0/\delta_b)\,[(\delta_a/\delta_b) - 1]. \tag{35}$$

According to the theory of large vortices which gives $U = 0.25\,u_m$, $r_{0b} = 0.22\,\delta_b$, and by virtue of equations (33) and (34), we have

$$V_{ai} = 0.012\,u_m \frac{A_0(\delta_a - \delta_b)}{a} = -V_{bi}(a/b). \tag{36}$$

The relationship between the total velocities of straining motion (32) and dimensions of the closed vortex field is expressed, according to equations (34) and (7), by

$$V_{a\Sigma} b = - V_{b\Sigma} a. \tag{37}$$

If the difference between the sides of the jet cross-section is large ($a \gg b$), the transitional segment on the shorter side terminates earlier than the initial segment on the longer side ($x_{trb} < x_{ia}$), but when $x_{trb} < x$ one should account for a change in the velocity on the jet axis ($u_m < u_1$) in the beginning by the laws of the plane-parallel jet and in the subsequent portion of the jet ($x > x_e$), by the laws of the 3-dim. jet.

As is known for a plane jet [2]

$$u_m/u_1 = (x_{trb}/x)^{1/2}. \tag{38}$$

For a rectangular jet at $x > x_e$, one can employ the law [7]

$$\frac{u_m}{u_1} = \frac{x_m}{x}, \tag{39}$$

where the abscissa x_m shows the place where the hyperbola (39) intersects the line $u_m = u_1$. The experiments described in ref. [7] show that for a tentative calculation of a rectangular turbulent jet one may assume that

$$x_m = 12.5\, R_0, \tag{40}$$

where R_0 is determined from equation (6).

The change-over from equation (38) to equation (39) is carried out on some intermediate abscissa $x_{e_t} \approx x_{tra}$, where the both functions intersect and therefore

$$x_{tra} \approx x_{e_t} = \frac{x_m^2}{x_{trb}}$$

or (41)

$$x_m = (x_{tra} x_{trb})^{1/2}.$$

The magnitudes of characteristic abscissas from equations (40) and (41) are used to determine the axial velocity of a rectangular jet.

The adequacy of equation (40) for the description of velocity distribution over the axis of a 3-dim. jet can be assessed from the spread of points in Fig. 6, where the results of all known experiments for rectangular jets

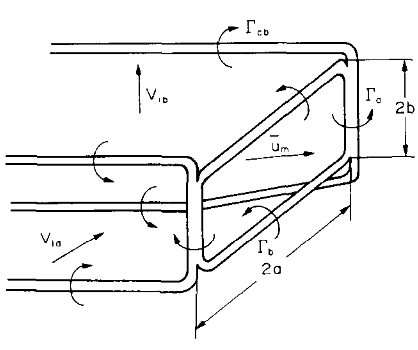

Fig. 5. A system of large vortices in a rectangular jet.

issuing both from smooth nozzles and sharp-edged orifices in a plane wall are presented.

The comparison between the predicted results and experimental data for each of the cases shown in Fig. 6 is given below.

When determining the difference of pressures by equation (4), we use the value of u_m obtained from equation (38) for the region $x_{tra} > x > x_{trb}$ and the value of u_m derived from equation (39) for the region $x > x_{tra}$.

The area of the vortex field R^2, assumed, in accordance with equation (6), to be constant over the starting jet portion (at $x < x_{ib}$) and increasing, according to equation (27), in the region $x > x_{ib}$, also grows in the main portion of the jet; here, both sides of the field increase with the jet thickness. According to equation (22), over the main portion of the jet (at $x > x_{ia}$)

$$R^2 = ab = 0.09\, \delta_a \delta_b. \tag{42}$$

At the same time, the vortex radius constitutes a constant fraction of the jet thickness

$$r_{0a} = 0.22\, \delta_a; \quad r_{0b} = 0.22\, \delta_b. \tag{43}$$

Hence, when the expressions (42) and (43) are substituted into equation (2), the same magnitude of the parameter q is obtained for the adjacent mixing layers ($q_a = q_b$), but then, according to equation (5), the difference of pressures on the adjacent sides of the vortex field disappears ($\Delta p = 0$). In such a case, at $x > x_{ia}$, the jet deformation depends only on the combination of the inertial rate of deformation V_a and the induced velocity V_{ai}

$$V_{a\Sigma} = V_a - V_{ai}. \tag{44}$$

Then

$$\frac{d^2 b}{dt^2} = \frac{-2V_{a\Sigma}^2}{b + (R^4/b^3)} \tag{45}$$

where V_{ia} is determined from equation (33).

It should be noted that in the region of the falling branch of the curve $u_m(x)$, the time interval corresponding to the computational step Δx, is determined taking into account the local value of u_m, i.e. according to equation (15) as

$$\Delta t = \frac{\Delta x}{u_0} = 1.43 \frac{\Delta x}{u_m}. \tag{46}$$

The above computational formulae are obtained for the case of a jet issuing from a nozzle with a uniform velocity field. The initial nonuniformity of the flow can be accounted for by substituting the real jet cross-section ($F_0 = R_0^2 = a_0 b_0$) for an equivalent one ($F_e = R_e^2 = a_e b_e$), in which the velocity is constant and equal to the maximum velocity on the axis at the origin of the real jet (u_1), while the total momentum is assumed to be the same. For lack of sufficient information on the initial velocity profiles in the reported experimental works, these corrections have not been introduced here.

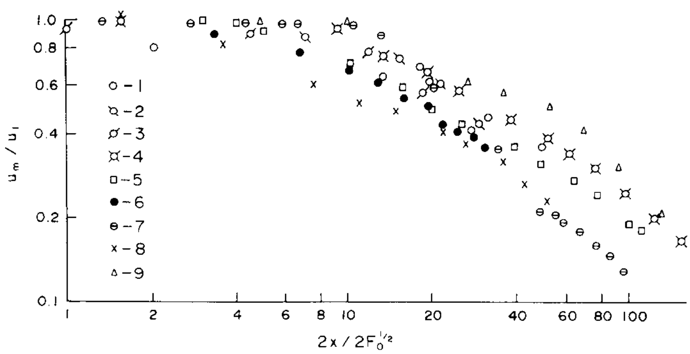

FIG. 6. Generalized curves of velocity attenuation along a rectangular jet axis at $n = a_0/b_0$ = var. Nozzles: 1, $n = 1$; 2, $n = 2$; 3, $n = 5$; 4, $n = 10$; 5, $n = 16.7$; 6, $n = 10$. Orifice: 7, $n = 5.25$; 8, $n = 12.4$; 9, $n = 10$.

In their experiments, Krashennikov *et al.* [7] and Krothapali *et al.* [15] studied the deformation of a jet issuing not only from a rectangular nozzle but also from a rectangular hole in a thin wall. It has been established that the jet discharge conditions influence appreciably the subsequent jet deformation. The initial compression of the jet coming out of a hole in a thin wall persists over a relatively small distance from the wall.

Let the sides of the constricted cross-section of a jet be a_K and b_K. The well-known solution for the problem of ideal fluid discharge from a thin wall, given in ref. [16] for a plane slot, as well as round and elliptical holes, shows that complete constriction of the jet in these cases is actually the same and equal to

$$\mu = R_K^2/R_0^2 \simeq 0.61. \quad (47)$$

A change in the jet cross-section $R^2 = ab$ over the length x is of an asymptotic nature, but the constriction of the cross-section area to the value $R_K^2 = 0.61\,R_0^2$ for a circle and a slot occurs at about the same distance from the wall

$$x_K = 1.6\,b_0, \quad (48)$$

where b_0 is the slot half-width (or the hole radius).

A rectangular hole occupies an intermediate position between an infinite slot and a square, while the behaviour of the compressed jet in the process of transition from one of these two cases to the other is similar to that which should be observed in the transition from an ellipse with an infinitely elongated major axis to a circle.

On the basis of what has been said above and in accordance with equation (47), the following relationship is adopted for the area of the constricted rectangular jet cross-section

$$R_K^2/R_0^2 = 0.61. \quad (49)$$

Then, for lack of a theoretical solution for the problem of rectangular jet constriction, it is assumed that over the constricted segment the side ratio remains constant, i.e.

$$a_K/a_0 = b_K/b_0. \quad (50)$$

Equations (49) and (50) yield the sides of the constricted cross-section

$$a_K = 0.79\,a_0; \quad b_K = 0.79\,b_0, \quad (51)$$

and, by analogy with equation (48), the distance from the wall to the constricted cross-section is

$$x_K = 1.6\,b_0. \quad (52)$$

Here, $2b_0$ is the small side of a rectangular hole.

Thus, accounting for the constriction of a jet as it issues from a slot in a thin wall is reduced to the replacement of the slot dimensions a_0, b_0 by a_K, b_K.

5. COMPARISON BETWEEN PREDICTION AND EXPERIMENT

When comparing the predicted results with the experimental data the following arguments have been applied.

It was shown experimentally by Krashennikov *et al.* that the dimensionless velocity profiles in the jet cross-sections along both symmetry axes are expressed by the same universal relationship, which is conventional for turbulent jets

$$\frac{u}{u_m} = f\left(\frac{y}{y_{0.5u}}\right) = f\left(\frac{z}{z_{0.5u}}\right)$$

where y and z are the coordinates of the instantaneous points on the symmetry axes of the cross-section; $y_{0.5u}$ and $z_{0.5u}$ are the same for the points at which the velocity is half that on the longitudinal jet axis ($u = 0.5\,u_m$). The use of the Shlichting velocity profile [2]

$$u/u_m = [1 - (y/\delta)^{3/2}]^2$$

shows that the values of $y_{0.5u}$ and $z_{0.5u}$ constitute the known fraction of the jet thickness

$$y_{0.5u}/\delta_a = z_{0.5u}/\delta_b = 0.415.$$

At the same time, it has been established in the theory of large vortices that the vortex axis is located at a constant relative distance from the maximum velocity line

$$a/\delta_a = b/\delta_b = 0.3.$$

Therefore, the conversion of the vortex field dimen-

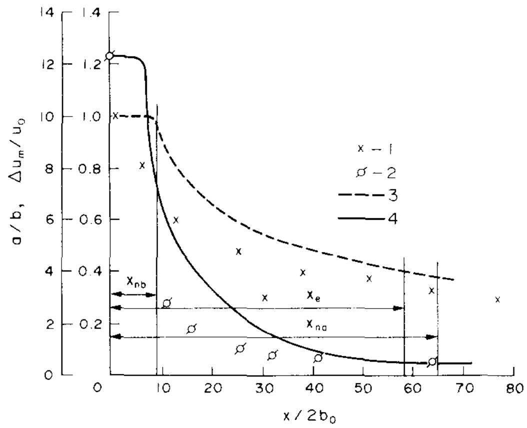

FIG. 7. Comparison between experiment and theory for a/b and u_m at $a_0/b_0 = 12.4$ (orifice). Experiment: 1, u_m; 2, a/b. Calculation: 3, u_m; 4, a/b.

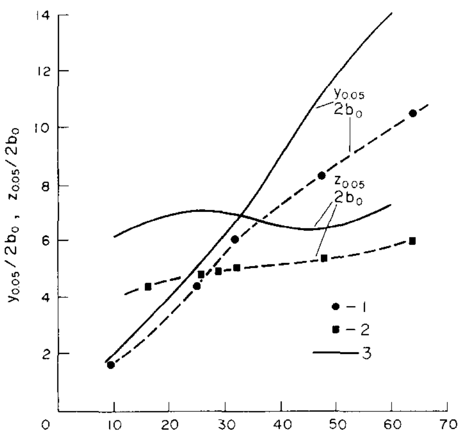

FIG. 8. Boundaries of a rectangular jet (orifice with $a_0 = 12.4\, b_0$): $y_{0.05u}/2b_0$, $z_{0.05u}/2a_0$. Experiment: 1, 2. Theory: 3.

sions b, a into characteristic jet dimensions $y_{0.5u}$, $z_{0.5u}$, determined experimentally, is carried out for the transitional and main portions of the jet as

$$z_{0.5u}/a = y_{0.5u}/b = 1.38; \quad a/b = z_{0.5u}/y_{0.5u}.$$

Figure 7 shows the comparison between the experimental data of Krashennikov *et al.* (points) and theoretical results (solid lines) for a jet issuing from a rectangular hole ($2a_0 = 62.5$ mm, $2b_0 = 5$ mm) in a plane wall (orifice). The initial degree of turbulence is about 2%, the jet discharge velocity varies in the range 40–90 m s^{-1}, which corresponds to a Reynolds number range of 1.5×10^4–6×10^4. Figure 7 shows the current value of the jet cross-section side ratio a/b plotted as abscissa and the corresponding dimensionless distance ($x/2b_0$) from the jet origin plotted as ordinate. The behaviour of the predicted curve $a/b = f(x/2b_0)$ agrees qualitatively with the position of experimental points, but is shifted somewhat to the right. This discrepancy can be explained by: (a) the presence of the boundary layer over the initial section of the jet with the resulting large finite vortices there, while it is assumed in calculations that the initial thickness of the mixing layer and the initial radius of the vortex are equal to zero; (b) the efflux from the orifice accompanied by initial constriction of the jet, which, in the case of a rectangular hole, can be an asymmetric one; the side ratio of this cross-section (a_K/b_K) may differ from that adopted for calculations.

Figure 8 compares the predicted and experimental coordinates $y/2b_0$ and $z/2a_0$ of the lines on which the velocity amounts to $0.05\, u_m$ for the same jet ($a_0 = 12.4\, b_0$).

Figure 9 shows the predicted and experimental results for the jet issuing from a smooth rectangular nozzle [14] with the dimensions of the outlet cross-section $2a_0 = 50$ mm, $2b_0 = 3$ mm ($a_0/b_0 = 16.7$) and

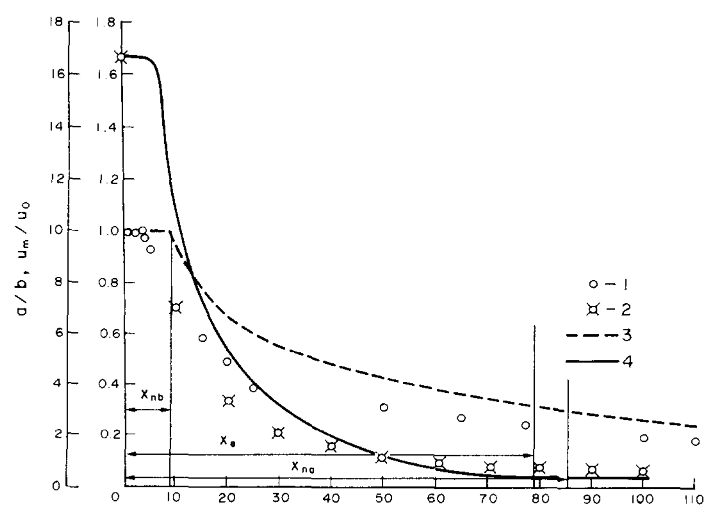

FIG. 9. Comparison between experiment and theory for a/b and u_m at $a_0 = 16.7\, b_0$ (nozzle). Experiment: 1, u_m; 2, a/b. Theory: 3, u_m; 4, a/b.

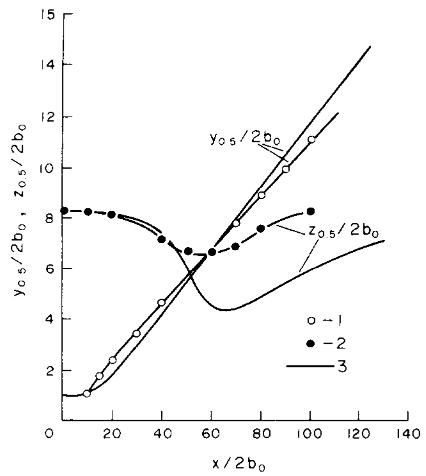

FIG. 10. Boundaries of a rectangular jet (nozzle with $a_0 = 16.7\, b_0$): $y_{0.5u}/2b_0$, $z_{0.5u}/2a_0$. Experiment: 1, 2. Theory: 3.

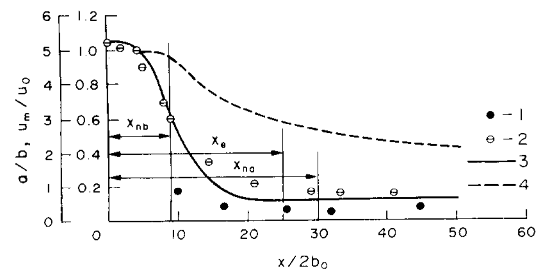

FIG. 12. Comparison between experiment and theory for a/b and u_m at $a_0/b_0 = 5.25$ (orifice). Experiment: 1, a/b; 2, u_m. Theory: 3, a/b; 4, experiment.

having the outlet section of constant area and the length of 40 mm. The nozzle had a large constriction and the level of turbulence at the jet origin amounted to 0.3% (at efflux velocities 60 m s^{-1} and the Reynolds numbers $Re = 1.2 \times 10^4$ based on the quantity $2b_0$). In Fig. 10, the predicted and experimental lines of the half-velocity ($y_{0.5u}/2b_0$; $z_{0.5u}/2a_0$) are given for the same jet ($a_0 = 16.7\, b_0$).

Figure 11 compares the experimental data of ref. [15] with the calculation carried out by the above technique for a rectangular jet, $a_0 = 10\, b_0$, in two versions: (a) the efflux from an orifice; (b) the efflux from a channel of the same cross-section ($2a_0 = 40$ mm; $2b_0 = 4$ mm) and of length $x_L = 200$ mm (the Reynolds number based on the linear dimension $2b_0 = 4$ mm is $Re = 12\,200$ for the turbulence level of 5% for the orifice and 3% for the channel).

Figure 12 presents the experimental curves $a/b = f(x/2b_0)$ compared with the predicted ones for the efflux from an orifice with $a_0 = 5.25\, b_0$.

Figures 7, 9, 11 and 12 show the behaviour of velocity u_m/u_1 along the jet axis as accepted in calculations (dashed line) and obtained in experiments.

6. CONCLUDING REMARKS

Thus, a hypothesis is advanced that in a mixing layer of a rectangular jet there exist discrete large vortices that move with an averaged flow velocity. The fluctuating superimposed flow moving past them creates a non-uniform pressure field which causes deformation of the jet cross-section. The calculation method developed agrees satisfactorily with the experiments.

Acknowledgement—The author would like to thank L. G. Golubtsova for great practical help with this work.

REFERENCES

1. V. A. Turkus, Structure of the air inflow jet issuing from a rectangular hole, *Zh. Otopl. Ventilyats.* No. 5, 11–19 (1933).
2. G. N. Abramovich, *Theory of Turbulent Jets.* Fizmatgiz, Moscow (1960).
3. E. Förthman, Über turbulente Strahlausbreitung, *Ing.-Arch.* **5**, 42–54 (1934).
4. M. L. Albertson, Y. B. Dai, R. A. Iensen and H. Rouse, Diffusion of submerged jets, *Proc. Am. Soc. civ. Engrs* **74**, 1751–1769 (1948).
5. M. P. Sforza, H. M. Steiger and N. Trentacoste, Studies on three-dimensional viscous jets, *AIAA J.* **4**, 800–806 (1966).
6. N. Trentacoste and M. P. Sforza, Further experimental results for three-dimensional free jets, *AIAA J.* **5**, 885–891 (1967).
7. S. Yu. Krashennikov and E. G. Rogalskaya, Propagation of jets from rectangular nozzles, free and those close to

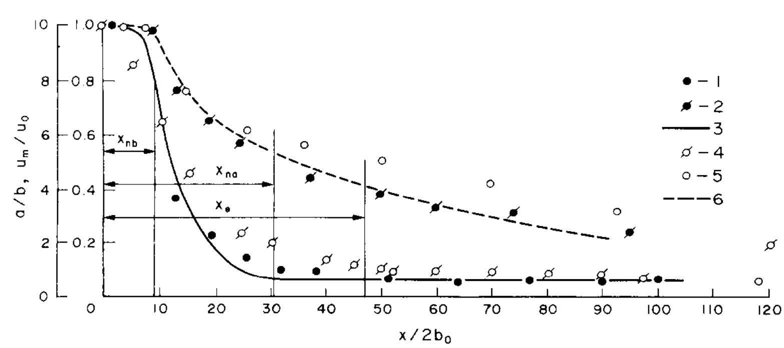

FIG. 11. Comparison between experiment and theory for a/b and u_m at $a_0 = 10\, b_0$. Orifice—experiment: 1, a/b; 2, u_m; theory: 3. Nozzle—experiment: 4, a/b; 5, u_m; theory: 3, a/b; 4, experiment.

the screen, *Izv. Akad. Nauk SSSR, Mekh. Zhid. Gaza* No. 4, 39–48 (1979).
8. J. J. McGriak and W. Rodi, The calculation of three-dimensional turbulent free jets, in *Symposium on Turbulent Shear Flows*, pp. 1–22. The Pennsylvania State University Press (1977).
9. A. Agulikov, K. E. Dzhaugashtin and L. P. Yarin, Study of the structure of three-dimensional turbulent jets, *Izv. Akad. Nauk SSSR, Mekh. Zhid. Gaza* No. 6, 13–21 (1975).
10. G. N. Abramovich, Effect of big vortices on the structure of turbulent shear flows, *Izv. Akad. Nauk SSSR, Mekh. Zhid. Gaza* No. 5, 10–20 (1979).
11. G. N. Abramovich, On propagation of pressure fluctuations in turbulent flows. Turbulent jet flows, in *Proc. 3rd All-Union Conf. on Theoretical and Applied Aspects of Turbulent Flows*, Pt. 1, pp. 5–19. Izv. Akad. Nauk Est. SSR, Tallin (1979).
12. G. N. Abramovich, On the long-range action of turbulent pressure fluctuations, in *Recent Developments in Theoretical and Experimental Fluid Mechanics*, pp. 467–479. Springer, Berlin (1979).
13. G. N. Abramovich, Effect of big vortices on the structure of turbulent shear flows, in *2nd Symposium on Turbulent Shear Flows*, 10.4–10.10. Imperial College Press, London (1979).
14. A. A. Sfeier, Investigation of three-dimensional turbulent rectangular jets, *AIAA 11th Fluid and Plasma Dynamics Conf.*, Vol. 1185, pp. 1–9 (1978).
15. A. Krothapali, D. Baganoff and K. Karamcheti, Turbulence measurements in a rectangular jet, *17th Aerospace Sciences Meeting*, pp. 1–19, New Orleans (1979).
16. G. Lamb, *Hydrodynamics*. Gostekhteorizdat, Moscow (1947).

SUR LA DEFORMATION DE LA SECTION DROITE D'UN JET TURBULENT RECTANGULAIRE

Résumé—On explique la raison de la déformation d'un jet turbulent rectangulaire qui apparait expérimentalement avec une croissance rapide (dans la direction du jet) du plus petit côté du jet et une reduction du plus grand côté. Ces changements sur les côtés prennent place à plusieurs distances en aval de l'origine du jet. La déformation est due à un champ de pression spécifique induit par de larges tourbillons qui apparaissent dans la zone de mélange du jet.

Une méthode de calcul de la déformation du jet est développée à partir de l'information de l'auteur sur le champ de pression produit par les grands tourbillons. Les résultats sont comparés avec données expérimentales en provenance d'autres sources. La théorie suggérée s'applique aux écoulements de jets dans les foyers de chaudière, les séchoirs, les chambres de combusion des réacteurs, les turbines à gaz terrestres des centrales électriques et les réacteurs chimiques, etc.

DEFORMATION EINES TURBULENTEN STRAHLES MIT RECHTECKQUERSCHNITT

Zusammenfassung—Dieser Aufsatz erklärt den Grund für die experimentell zu beobachtende Deformation eines turbulenten Strahls von rechteckigem Querschnitt, die sich in einem schnellen Anwachsen (in Strahlrichtung) der kürzeren Rechteckseite und einer Verkleinerung der größeren Seite äußert. Schließlich vertauschen die beiden Seiten in einer gewissen Entfernung vom Strahlanfang ihre Plätze. Es zeigt sich, daß die Strahl-Deformation durch ein spezifisches Druckfeld hervorgerufen wird, das durch große Wirbel induziert ist, die aus der Mischzone des Strahls stammen. Zur Berechnung der Strahl-Deformation wird ein Verfahren entwickelt, das von Informationen des Autors über wirbelinduzierte Druckfelder Gebrauch macht. Die Ergebnisse werden mit Versuchsdaten aus anderen Quellen verglichen. Die vorgeschlagene Theorie läßt sich auf Strahlströmungen anwenden, wie sie in Kesseln, Trocknern, Brennkammern von Strahl-Triebwerken und von stationären Gasturbinen, chemischen Reaktoren usw. vorkommen.

О ДЕФОРМАЦИИ ПОПЕРЕЧНОГО СЕЧЕНИЯ ПРЯМОУГОЛЬНОЙ ТУРБУЛЕНТНОЙ СТРУИ

Аннотация—В работе объясняется причина наблюдающейся в опытах деформации прямоугольной турбулентной струи, выражающейся в быстром росте (по длине струи) короткой стороны поперечного сечения и уменьшении длинной его стороны. В результате такой перестройки на некотором расстоянии от начала струи короткая и длинная стороны поперечного сечения струи меняются местами. Показывается, что деформация струи вызывается специфическим полем давления, которое индуцируется крупными вихрями, возникающими в зоне смешения струи.

Разработан метод расчета деформации струи, использующий сведения о поле давления, создаваемом крупными вихрями, заимствуемые из работ автора. Результаты расчета сопоставляются с экспериментальными данными других авторов. Предлагаемая теория приложима к расчету струйных течений в топках котельных устройств, сушилках, камерах сгорания реактивных двигателей и стационарных газотурбинных установок электростанций, химических реакторах и др.